Designing and Studying Darboux Sweeping Surface in Isotropic Space I_3^1

W. M. MAHMOUD[1], ESRAA. M. MOHAMED[1], M. A. SOLIMAN[2]
[1]Department of Mathematics, Faculty of Science,
Aswan University, Aswan, EGYPT

[2]Department of Mathematics, Faculty of Science,
Assiut University, Assiut, EGYPT

Abstract: - This research aims to study Darboux sweeping surface in isotropic space I_1^3. We went through the geometric characteristics of sweeping surfaces in I_1^3 . The first and second fundamental forms of the sweeping surface were evaluated. Furthermore, we investigate the mean and Gaussian curvature of the sweeping surface. We also show that the parametric curves on these surfaces are non-geodesic and non-asymptotic. Then, we derive the necessary and sufficient conditions for the sweeping surface to become a developable sweeping surface, minimal sweeping surface, and Weingarten surface. Finally, an example to illustrate the application of the results is introduced.

Key-Words: - Sweeping surface; Darboux frame; isotropic space; Weingarten sweeping surface; minimal sweeping surface; developable sweeping surface

Received: October 21, 2022. Revised: February 18, 2023. Accepted: March 14, 2023. Published: April 12, 2023.

1 Introduction

Both the kinematics and differential line geometry theory, considering sweeping surfaces asIn both the kinematics and differential line geometry theory considering sweeping surfaces as special ruled surfaces are critical. A canal channel surface is etched out as the envelope of a one-parameter family of spheres, the spine or directory, with their centers on a space curve: The canal surface, also known as a sweeping or pipe surface, is the envelope of a moving sphere when the generating spheres' radii are constant. The right circular cylinder (spine is a line, the axis of the cylinder), a torus (directory is a circle), right circular cone (spine is a line (the axis), radii of the spheres not constant), and the surface of revolution are all examples that we are familiar with (spine is a line). This idea is a broadening of the idea of a planar curve's mate, [1], [2]. Sweeping surfaces are used in a variety of applications in Computer Aided Geometric Design (CAGD), including robotic path planning, blending surfaces, pipe transition surfaces, and sculptured surface production, [3], [4]. A sweeping surface is generated in space by the motion of a plane curve (the profile curve or generatrix), with the plane migrating in the same direction as the plane's normal. Sweeping is a useful and vital tool in geometrical modelling, with certain applications in geometric design. The concept is based on selecting a geometrical object, known as a generator, and sweeping it along a spine curve, known as a trajectory, [5], [6], [7]. In recent years, researchers have explored the characteristics of sweeping surfaces and their offset surfaces in both Euclidean and non-Euclidean spaces, [8], [9]. The many names for sweeping surfaces include tubular surface, pipe surface, string surface, and canal surface, according to the references, [9], [10], [3]. This research focuses on the geometrical properties of sweeping surfaces whose canter curves in surfaces in isotropic 3-space I_3^1 . Furthermore, sweeping surfaces, often referred to as ruled surfaces, are key components of line trajectory and are represented in kinematics as one-dimensional line manifolds created by directed moving lines in space, [2].

In this work, the sweeping surface's differential geometry is created in isotropic 3-space using the Darboux frame. The parametric curves on this surface are also shown to be non-geodesic and non-asymptotic. We found the necessary and sufficient criteria for a sweeping surface to become a minimal and developable sweeping surface and a Weingarten surface. Finally, an example is introduced to show how the findings are used.

2 Preliminaries

Isotropic space based on the following group G_6 of affine transformation (so-called isotropic congruence transformations or $i-$motions) is a Cayley-Klein space, it is based on the slave orchestrate G_6 of an affine transformation$(\mathcal{A},\mathcal{B},\mathcal{C}) \rightarrow (\bar{\mathcal{A}},\bar{\mathcal{B}},\bar{\mathcal{C}})$ in $\mathbb{R}^3$.

$$\begin{aligned}\bar{\boldsymbol{\mathcal{A}}} &= \boldsymbol{r_1} + \boldsymbol{\mathcal{A}}\cos(\mathfrak{S}) - \boldsymbol{\mathcal{B}}\sin(\mathfrak{S})\\ \bar{\boldsymbol{\mathcal{B}}} &= \boldsymbol{r_2} + \boldsymbol{\mathcal{A}}\sin(\mathfrak{S}) + \boldsymbol{\mathcal{B}}\cos(\mathfrak{S})\\ \bar{\boldsymbol{\mathcal{C}}} &= \boldsymbol{r_3} + \boldsymbol{r_4}\,\boldsymbol{\mathcal{A}} + \boldsymbol{r_5}\,\boldsymbol{\mathcal{B}} + \boldsymbol{\mathcal{C}},\end{aligned} \tag{1}$$

where r_1 , r_2 , r_3 , r_4 , r_5 , $\mathfrak{S} \in \mathbb{R}$.

Affine transformations include isotropic congruence transformations or isotropic movements. Isotropic distance between two points The Euclidean distance is defined by $\mathcal{J} = (q_1, t_1, s_1)$ and $\mathcal{T} = (q_2, t_2, s_2)$

$$d(\mathcal{J},\mathcal{T}) = \sqrt{(q_1 - q_2)^2 + (t_1 - t_2)^2}$$

Let $\alpha = (q_1, t_1, s_1)$ and $\beta = (q_2, t_2, s_2)$ be vectors in I_1^3 . The isotropic inner product of α and β is defined by.

$$\langle \boldsymbol{\alpha},\boldsymbol{\beta}\rangle = \begin{cases} \boldsymbol{s_1 s_2} & \boldsymbol{if\ q_i = t_i = 0} \\ \boldsymbol{q_1 q_2 + t_1 t_2} & \boldsymbol{if\ otherwise} \end{cases} \tag{2}$$

we consider $\{\varrho_1, \varrho_2, \varrho_3\}$ and $\{\lambda_1, \lambda_2, \lambda_3\}$to be the Serret Frenet frame and Darboux frame associated with the curve $\mu(\mathfrak{L})$ respectively, the Serret Frenet formulas are as follows:

$$\begin{cases} \dfrac{d\varrho_1}{d\mathfrak{L}} = \kappa(\mathfrak{L})\,\varrho_2(\mathfrak{L}), \\ \dfrac{d\varrho_2}{d\mathfrak{L}} = -\kappa(\mathfrak{L})\,\varrho_1(\mathfrak{L}) + \tau\,\varrho_3(\mathfrak{L}), \\ \dfrac{d\varrho_3}{d\mathfrak{L}} = -\tau\,\varrho_2(\mathfrak{L}) \end{cases} \tag{3}$$

where $\varrho_1(\mathfrak{L}) = \acute{\mu}(\mathfrak{L})$ denotes unit tangent, $\varrho_2(\mathfrak{L}) = \frac{\acute{\mu(\mathfrak{L})}}{\|\acute{\mu(\mathfrak{L})}\|}$ defines the unit principal normal, and $\varrho_3(\mathfrak{L}) = \varrho_1(\mathfrak{L}) \times \varrho_2(\mathfrak{L})$ defines a unit binormal vector and

$$\begin{aligned}\boldsymbol{h(\varrho_1,\varrho_1) = h(\varrho_2,\varrho_2) = h(\varrho_3,\varrho_3) = 1}\\ \boldsymbol{h(\varrho_1,\varrho_2) = h(\varrho_2,\varrho_3) = h(\varrho_1,\varrho_3) = 0}\end{aligned} \tag{4}$$

Also, consider $\mu : I \rightarrow I_1^3$ as a regular curve with $\acute{\mu} = \frac{dx}{dt} \neq 0$. If μ has a unit tangent vector field, unit principal normal vector field, and unit binormal vector field as λ_1, λ_2 and λ_3 respectively. The Darboux frame is defined by λ_1, λ_2 and λ_3 , its formulas are provided by

$$\begin{bmatrix} \acute{\lambda_1} \\ \acute{\lambda_2} \\ \acute{\lambda_3} \end{bmatrix} = \begin{bmatrix} \mathbf{0} & \boldsymbol{\kappa_g} & \boldsymbol{\tau_g} \\ -\boldsymbol{\kappa_g} & \mathbf{0} & \boldsymbol{\tau_g} \\ -\boldsymbol{\kappa_n} & -\boldsymbol{\tau_g} & \mathbf{0} \end{bmatrix} \begin{bmatrix} \lambda_1 \\ \lambda_2 \\ \lambda_3 \end{bmatrix} \tag{5}$$

Where

$$\begin{cases} \kappa_n = \kappa(\mathfrak{L})\,sin\,(\Psi), \\ \kappa_g = \kappa(\mathfrak{L})\,cos\,(\Psi), \\ \tau_g = \tau + \acute{\Psi} \end{cases} \tag{6}$$

Where κ_g , κ_n and τ_g are the geodesic curvature, the normal curvature, and the geodesic torsion of $\mu(\mathfrak{L})$ and

$$\begin{aligned}\boldsymbol{h(\lambda_1,\lambda_1) = h(\lambda_2,\lambda_2) = h(\lambda_3,\lambda_3)} &= \mathbf{1}\\ \boldsymbol{h(\lambda_1,\lambda_2) = h(\lambda_2,\lambda_3) = h(\lambda_1,\lambda_3)} &= \mathbf{0}\end{aligned} \tag{7}$$

This formula illustrates the relationship between Serret–Frenet frame and the Darboux frame

$$\begin{bmatrix} \boldsymbol{\varrho_1} \\ \boldsymbol{\varrho_2} \\ \boldsymbol{\varrho_3} \end{bmatrix} = \begin{bmatrix} \mathbf{1} & \mathbf{0} & \mathbf{0} \\ \mathbf{0} & \boldsymbol{cos}\,(\mathfrak{G}) & \mathbf{sin}(\mathfrak{G}) \\ \mathbf{0} & -\mathbf{sin}(\mathfrak{G}) & \boldsymbol{cos}\,(\mathfrak{G}) \end{bmatrix} \begin{bmatrix} \lambda_1 \\ \lambda_2 \\ \lambda_3 \end{bmatrix} \tag{8}$$

Isotropic curvature and isotropic torsion of μ are represented by κ and τ, respectively. If there are no isotropic tangent planes on a surface $\mathfrak{D}$ submerged in I_1^3, the surface is said to be admissible.
A surface χ in I_1^3 by ,

$$\boldsymbol{\chi(\mathfrak{L},\mathfrak{S})} = \boldsymbol{(\chi_1(\mathfrak{L},\mathfrak{S}), \chi_2\,(\mathfrak{L},\mathfrak{S}), \chi_3(\mathfrak{L},\mathfrak{S}))} \tag{9}$$

The coefficients $\mathcal{P}_{11}$, $\mathcal{P}_{12}$, $\mathcal{P}_{22}$ of 1st fundamental form for the induced metric and the coefficients $\mathcal{F}_{11}, \mathcal{F}_{12}, \mathcal{F}_{22}$ of 2nd fundamental form for the normal vector field are obtained for a surface that is always completely isotropic.

$$\begin{aligned}\boldsymbol{I} &= \boldsymbol{\mathcal{P}_{11}\,d\mathfrak{L}^2 + \mathcal{P}_{12}\,d\mathfrak{L}\,d\mathfrak{S}}\\ &\quad \boldsymbol{+ \mathcal{P}_{22}\,d\mathfrak{S}^2},\\ \boldsymbol{I\,I} &= \boldsymbol{\mathcal{F}_{11}d\mathfrak{L}^2 + \mathcal{F}_{12}\,d\mathfrak{L}d\mathfrak{S}}\\ &\quad \boldsymbol{+ \mathcal{F}_{22}\,d\mathfrak{S}^2}\end{aligned} \tag{10}$$

where

$$\boldsymbol{\mathcal{P}_{11}} = \langle \boldsymbol{\chi_{\mathfrak{L}}, \chi_{\mathfrak{L}}}\rangle, \boldsymbol{\mathcal{P}_{12}} = \langle \boldsymbol{\chi_{\mathfrak{L}}, \chi_{\mathfrak{S}}}\rangle, \boldsymbol{\mathcal{P}_{22}} = \langle \boldsymbol{\chi_{\mathfrak{L}}, \chi_{\mathfrak{S}}}\rangle \tag{11}$$

$$\mathcal{F}_{11} = \langle \chi_{\mathfrak{L}\mathfrak{L}}, \mathcal{O}\rangle,\ \mathcal{F}_{12} = \langle \chi_{\mathfrak{L}\mathfrak{S}}, \mathcal{O}\rangle,\ \mathcal{F}_{22} = \langle \chi_{\mathfrak{S}\mathfrak{S}}, \mathcal{O}\rangle \tag{12}$$

$\mathcal{O}$ = (0, 0, 1) denotes the isotropic unit normal vector field. The Gaussian curvature $\mathcal{K}$ and mean curvature $\mathcal{H}$ are defined by using the classical notation above.

$$\boldsymbol{\mathcal{K}} = \frac{\boldsymbol{\mathcal{F}_{11}\mathcal{F}_{22} - \mathcal{F}_{12}^2}}{\boldsymbol{\mathcal{P}_{11}\mathcal{P}_{22} - \mathcal{P}_{12}^2}} \quad ,$$

$$\mathcal{H} = \frac{\mathcal{P}_{11}\mathcal{F}_{22} - 2\,\mathcal{P}_{12}\mathcal{F}_{12} + \mathcal{F}_{11}\mathcal{P}_{22}}{\mathcal{P}_{11}\,\mathcal{P}_{22} - \mathcal{P}_{12}{}^{2}}$$

The surface $\mathfrak{D}$ is said to be isotropic flat if $\mathcal{K}$ (resp. $\mathcal{H}$) vanishes (resp. isotropic minimal), [11], [12], [13], [14].

3 Darboux Sweeping Surfaces' Geometric Properties in Isotropic 3-Space

Let $\mathfrak{D}$ be a sweeping surface in isotropic 3-space I_3^1 is given by

$$\mathfrak{D}: \boldsymbol{\chi}(\mathfrak{L}, \mathfrak{S}) = \mu(\mathfrak{L}) + \boldsymbol{X}(\mathfrak{S}) \tag{13}$$

Where $\mu(\mathfrak{L})$ is the spine curve of the surface $\mathfrak{D}$. The envelope of the family of unit spheres with the center on the curve $\mu(\mathfrak{L})$ is represented by the sweeping surface associated with $\mu(\mathfrak{L}) \in \mathfrak{S}$. we have

$$\boldsymbol{X}(\mathfrak{S}) = \boldsymbol{cos}(\mathfrak{S})\,\lambda_2 + \boldsymbol{sin}(\mathfrak{S})\,\lambda_3 \tag{14}$$

This is the typical sweeping surface circle. When we combine Eqs. (13) and (14), we get a parameterization of the sweeping surface

$$\begin{aligned}\mathfrak{D}: \boldsymbol{\chi}(\mathfrak{L}, \mathfrak{S}) &= \mu(\mathfrak{L}) \\ &+ \mathbf{cos}(\mathfrak{S})\lambda_2 \\ &+ \mathbf{sin}(\mathfrak{S})\lambda_3\end{aligned} \tag{15}$$

This parameterization of $\mathfrak{D}$ eliminates sweeping surfaces with stationary vectors since their geometrical features are not particularly relevant and are easily explored.

The characteristics of sweeping surfaces. We compute using the formulas in Eq. (15).

$$\begin{aligned}\boldsymbol{\chi}_{\mathfrak{L}}(\mathfrak{L}, \mathfrak{S}) &= (\mathbf{1} - \mathbf{cos}(\mathfrak{S})\,\boldsymbol{\kappa}_g(\mathfrak{L}) \\ &- \boldsymbol{Sin}(\mathfrak{S})\boldsymbol{\kappa}_n(\mathfrak{L}))\lambda_1 \\ &- \boldsymbol{Sin}(\mathfrak{S})\boldsymbol{\tau}_g(\mathfrak{L})\lambda_2 \\ &+ \mathbf{cos}(\mathfrak{S})\,\boldsymbol{\tau}_g(\mathfrak{L})\lambda_3\end{aligned} \tag{16}$$

$$\begin{aligned}\chi_{\mathfrak{S}}(\mathfrak{L}, \mathfrak{S}) &= -Sin(\mathfrak{S})\lambda_2 \\ &+ \cos(\mathfrak{S})\,\lambda_3\end{aligned} \tag{17}$$

$$\mathcal{O}(\mathfrak{L}, \mathfrak{S}) = (0, 0, 1) \tag{18}$$

Eq. (18) shows that the surface normal $\mathcal{O}(\mathfrak{L}, \mathfrak{S})$, Also Eq. (11), (16), and (17), It is straightforward to show that the coefficients of the first fundamental form are obtained by

$$\begin{aligned}&\boldsymbol{\mathcal{P}_{11}} = (-\mathbf{1} + \\ &\mathbf{cos}(\mathfrak{S})\boldsymbol{\kappa}_g(\mathfrak{L}) + \mathbf{sin}(\mathfrak{S})\boldsymbol{\kappa}_n(\mathfrak{L}))^2 + \\ &\mathbf{sin}^2(\mathfrak{S})\,\boldsymbol{\tau}_g(\mathfrak{L})^2, \\ &\boldsymbol{\mathcal{P}_{12}} = \mathbf{sin}^2(\mathfrak{S})\,\boldsymbol{\tau}_g(\mathfrak{L}). \\ &\boldsymbol{\mathcal{P}_{22}} = \mathbf{sin}^2(\mathfrak{S})\end{aligned} \tag{19}$$

To compute the 2nd fundamental form of $\mathfrak{D}$, The following equation must be calculated.

$$\begin{aligned}\boldsymbol{\chi}_{\mathfrak{L}\mathfrak{L}}(\mathfrak{L}, \mathfrak{S}) &= \big(\mathbf{sin}(\mathfrak{S})\,\boldsymbol{k}_g(\mathfrak{L})\boldsymbol{\tau}_g(\mathfrak{L}) \\ &- \mathbf{cos}(\mathfrak{S})\big(\boldsymbol{k}_n(\mathfrak{L})\boldsymbol{\tau}_g(\mathfrak{L}) \\ &+ \boldsymbol{k}_g'(\mathfrak{L})\big) \\ &- \mathbf{sin}(\mathfrak{S})\,\boldsymbol{k}_n{}'(\mathfrak{L})\big)\lambda_1 \\ &+ \Big(\boldsymbol{k}_g(\mathfrak{L}) - \mathbf{cos}(\mathfrak{S})\big(\boldsymbol{k}_g(\mathfrak{L})^2 + \boldsymbol{\tau}_g(\mathfrak{L})^2\big) \\ &- \mathbf{sin}(\mathfrak{S})\big(\boldsymbol{k}_g(\mathfrak{L})\boldsymbol{k}_n(\mathfrak{L}) \\ &+ \boldsymbol{\tau}_g'(\mathfrak{L})\big)\Big)\lambda_2 \\ &+ \Big(\boldsymbol{k}_n(\mathfrak{L}) - \mathbf{sin}(\mathfrak{S})\big(\boldsymbol{k}_n(\mathfrak{L})^2 + \boldsymbol{\tau}_g(\mathfrak{L})^2\big) \\ &+ \mathbf{cos}(\mathfrak{S})\Big(-\boldsymbol{k}_g(\mathfrak{L})\boldsymbol{k}_n(\mathfrak{L}) + \boldsymbol{\tau}_g'(\mathfrak{L})\Big)\Big)\lambda_3\end{aligned} \tag{20}$$

$$\begin{aligned}\boldsymbol{\chi}_{\mathfrak{S}\mathfrak{S}}(\mathfrak{L}, \mathfrak{S}) &= (-\mathbf{cos}(\mathfrak{S}))\lambda_2 \\ &+ (-\mathbf{sin}(\mathfrak{S}))\lambda_3\end{aligned}$$

$$\begin{aligned}\boldsymbol{\chi}_{\mathfrak{L}\mathfrak{S}}(\mathfrak{L}, \mathfrak{S}) &= \big(\mathbf{sin}(\mathfrak{S})\,\boldsymbol{k}_g(\mathfrak{L}) \\ &- \mathbf{cos}(\mathfrak{S})\,\boldsymbol{k}_n(\mathfrak{L})\big)\lambda_1 \\ &+ \big(-\mathbf{cos}(\mathfrak{S})\,\boldsymbol{\tau}_g(\mathfrak{L})\big)\lambda_2 \\ &+ \big(-\mathbf{sin}(\mathfrak{S})\,\boldsymbol{\tau}_g(\mathfrak{L})\big)\lambda_3\end{aligned}$$

From Eqs. (12), (18), and (20) provide 2nd fundamental form elements as given by

$$\begin{aligned}&\boldsymbol{\mathcal{F}_{11}} \\ &= \boldsymbol{k}_n(\mathfrak{L}) - \mathbf{sin}(\mathfrak{S})\big(\boldsymbol{k}_n(\mathfrak{L})^2 + \boldsymbol{\tau}_g(\mathfrak{L})^2\big) \\ &+ \mathbf{cos}(\mathfrak{S})\Big(-\boldsymbol{k}_g(\mathfrak{L})\boldsymbol{k}_n(\mathfrak{L}) + \boldsymbol{\tau}_g'(\mathfrak{L})\Big), \\ &\boldsymbol{\mathcal{F}_{12}} = -\mathbf{sin}(\mathfrak{S})\,\boldsymbol{\tau}_g(\mathfrak{L}), \\ &\boldsymbol{\mathcal{F}_{22}} = -\mathbf{sin}(\mathfrak{S}).\end{aligned} \tag{21}$$

The Gaussian and mean curvature of the Darboux sweeping surface at a regular point may be found as follows:

$$\begin{aligned}&\boldsymbol{\mathcal{K}}(\mathfrak{L}, \mathfrak{S}) = \\ &\frac{\mathbf{csc}(\mathfrak{S})}{\Big(-\mathbf{1} + \mathbf{cos}(\mathfrak{S})\,\boldsymbol{k}_g(\mathfrak{L}) + \mathbf{sin}(\mathfrak{S})\,\boldsymbol{k}_n(\mathfrak{L})\Big)^2} \\ &\big((-\mathbf{1} + \mathbf{cos}(\mathfrak{S})\,\boldsymbol{k}_g(\mathfrak{L}))\boldsymbol{k}_n(\mathfrak{L}) \\ &+ \mathbf{sin}(\mathfrak{S})\,\boldsymbol{k}_n(\mathfrak{L})^2 \\ &- \mathbf{cos}(\mathfrak{S})\,\boldsymbol{\tau}_g'(\mathfrak{L})\big)\end{aligned} \tag{22}$$

$$\begin{aligned}&\mathcal{H}(\mathfrak{L}, \mathfrak{S}) = \\ &-\frac{\csc(\mathfrak{S})}{2\Big(-\csc(\mathfrak{S}) + \cot(\mathfrak{S})\,k_g(\mathfrak{L}) + k_n(\mathfrak{L})\Big)^2} \\ &\big(\csc(\mathfrak{S})^2 + \cot(\mathfrak{S})^2\,k_g(\mathfrak{L})^2 \\ &- 3\,\csc(\mathfrak{S})\,k_n(\mathfrak{L}) + 2k_n(\mathfrak{L})^2 \\ &- \cot(\mathfrak{S})\csc(\mathfrak{S})\,k_g(\mathfrak{L})(-2 \\ &+ 3\,\sin(\mathfrak{S})\,k_n(\mathfrak{L})) - \cot(\mathfrak{S})\,\tau_g'(\mathfrak{L})\big)\end{aligned} \tag{23}$$

Proposition 3.1 The sweeping surface $\mathfrak{D}$ is represented by Eq. (15), thus we can say:

1. When μ is a geodesic on $\mathfrak{D}$, then the sweeping surface $\mathfrak{D}$'s Gaussian and mean curvature are:

$$\boldsymbol{\mathcal{K}(\mathfrak{L},\ \mathfrak{S})} = \frac{\mathbf{csc(\mathfrak{S})}}{\mathbf{(-1+\sin(\mathfrak{S})\,k_n(\mathfrak{L}))^2}}\left(\mathbf{-k_n(\mathfrak{L})} + \mathbf{\sin(\mathfrak{S})\,k_n(\mathfrak{L})^2 - \cos(\mathfrak{S})\,\tau_g'(\mathfrak{L})}\right) \quad (24)$$

$$\mathcal{H}(\mathfrak{L},\ \mathfrak{S}) = -\frac{\csc(\mathfrak{S})}{2\left(-\csc(\mathfrak{S})+k_n(\mathfrak{L})\right)^2}\left(-k_n(\mathfrak{L})+\sin(\mathfrak{S})\,k_n(\mathfrak{L})^2-\cos(\mathfrak{S})\,\tau_g'(\mathfrak{L})\right) \quad (25)$$

2. The Gaussian and mean curvature of the sweeping surface $\mathfrak{D}$ are found if μ is an asymptotic on $\mathfrak{D}$.

$$\boldsymbol{\mathcal{K}(\mathfrak{L},\ \mathfrak{S})} = -\frac{\mathbf{\cot(\mathfrak{S})\,\tau_g'(\mathfrak{L})}}{\mathbf{(-1+\cos(\mathfrak{S})\,k_g(\mathfrak{L}))^2}} \quad (26)$$

$$\mathcal{H}(\mathfrak{L},\ \mathfrak{S}) = -\frac{\csc(\mathfrak{S})}{2\left(-\csc(\mathfrak{S})+\cot(\mathfrak{S})\,k_g(\mathfrak{L})\right)^2}\left(\csc(\mathfrak{S})^2-2\cot(\mathfrak{S})\csc(\mathfrak{S})\,k_g(\mathfrak{L})+\cot(\mathfrak{S})^2\,k_g(\mathfrak{L})^2-\cot(\mathfrak{S})\,\tau_g'(\mathfrak{L})\right) \quad (27)$$

On the other side, Eq. (15) clearly shows that the isoperimetric curve exists.

Theorem 3.2 Let $\chi(\mathfrak{L},\mathfrak{S})$ be Daurbox sweeping surface in an isotropic 3-space. Then the followings are satisfied:

1. $\mathfrak{S}$-parameter curves of the surface are non-asymptotic curves.

2. $\mathfrak{S}$-parameter curves of the surface are non-geodesic curves.

proof: Suppose that $\chi(\mathfrak{L},\mathfrak{S})$ is a sweeping surface such that $\chi(\mathfrak{L},\mathfrak{S})$ is a unit speed curve for all $\mathfrak{S}$. It is well known $k_n(\mathfrak{L})$ of a $\mathfrak{S}$-parameter curve on the surface $\chi(\mathfrak{L},\mathfrak{S})$ is given by

$$k_n(\mathfrak{L}) = \langle \mathcal{O}, \chi_{\mathfrak{S}\mathfrak{S}}\rangle = -sin(\mathfrak{S})$$

$$\kappa_g(\mathfrak{L}) = \langle \mathcal{O}\times\chi_{\mathfrak{S}}, \chi_{\mathfrak{S}\mathfrak{S}}\rangle = -sin(\mathfrak{S})\cos(\mathfrak{S})$$

Thus, A. $\mathfrak{S}$-parameter curve is non-asymptotic and non-geodesic.

Theorem 3.3 The sweeping surface $\mathfrak{D}$ according to Darboux frame in isotropic 3-space is developable if and only if

$$k_n(\mathfrak{L}) = \frac{1}{2}\csc(\mathfrak{S})\,(1-\cos(\mathfrak{S})\,k_g(\mathfrak{L}) \pm \sqrt{(-1+\cos(\mathfrak{S})\,k_g(\mathfrak{L}))^2+4\cos(\mathfrak{S})\sin(\mathfrak{S})\,\tau_g'(\mathfrak{L})}$$

proof: The sweeping μ$(\mathfrak{L},\mathfrak{S})$ if and only if $\mathcal{K}(\mathfrak{L},\mathfrak{S}) = 0$ From the Eq. (22) we have $csc(\mathfrak{S}) \neq 0$ and $\left(-1+\cos(\mathfrak{S})\,k_g(\mathfrak{L})\right)k_n(\mathfrak{L})+\sin(\mathfrak{S})\,k_n(\mathfrak{L})^2-\cos(\mathfrak{S})\,\tau_g'(\mathfrak{L}))=0$, we get

$$k_n(\mathfrak{L}) = \frac{1}{2}\csc(\mathfrak{S})\,(1-\cos(\mathfrak{S})\,k_g(\mathfrak{L}) \pm \sqrt{(-1+\cos(\mathfrak{S})\,k_g(\mathfrak{L}))^2+4\cos(\mathfrak{S})\sin(\mathfrak{S})\,\tau_g'(\mathfrak{L})}$$

Then the surface $\mathfrak{D}$ is developable.

Theorem 3.4 The sweeping surface $\mathfrak{D}$ according to Darboux frame in isotropic 3-space is Weingarten sweeping surface if and only if:

$$\mathcal{H}_{\mathfrak{L}}\mathcal{K}_{\mathfrak{S}} = \mathcal{H}_{\mathfrak{S}}\mathcal{K}_{\mathfrak{L}}$$

proof: from the Eqs. (22) and (23) we have

$$\mathcal{H}_{\mathfrak{L}} = \frac{\csc(\mathfrak{S})}{2\left(\csc(\mathfrak{S})-\cot(\mathfrak{S})\,k_g(\mathfrak{L})-k_n(\mathfrak{L})\right)^3}\Big(\Big(-\cot(\mathfrak{S})\,k_n(\mathfrak{L})^2k_g'(\mathfrak{L})+k_n'(\mathfrak{L})\left(\csc(\mathfrak{S})-\cot(\mathfrak{S})\,k_g(\mathfrak{L})\right)^2+2\cot(\mathfrak{S})\,\tau_g'(\mathfrak{L})\Big)+\left(k_n(\mathfrak{L})((\csc(\mathfrak{S})-\cot(\mathfrak{S})\,k_g(\mathfrak{L}))(\cot(\mathfrak{S})\,k_g'(\mathfrak{L})-k_n'(\mathfrak{L}))\right)+\left(-\cot(\mathfrak{S})\,\tau_g''(\mathfrak{L})+\cot(\mathfrak{S})\,(2\cot(\mathfrak{S})\,k_g'(\mathfrak{L})\tau_g'(\mathfrak{L})\right)+(2\cot(\mathfrak{S})\,k_g'(\mathfrak{L})\tau_g'(\mathfrak{L})+(\csc(\mathfrak{S})-\cot(\mathfrak{S})\,k_g(\mathfrak{L}))\tau_g''(\mathfrak{L}))\Big)$$

$$\mathcal{H}_{\mathfrak{S}} = \frac{1}{2}\Bigg(\cot(\mathfrak{S})\csc(\mathfrak{S}) - \frac{\sin(\mathfrak{S})\,k_g(\mathfrak{L})k_n(\mathfrak{L})}{\left(-1+\cos(\mathfrak{S})\,k_g(\mathfrak{L})+\sin(\mathfrak{S})\,k_n(\mathfrak{L})\right)^2} + \frac{\cos(\mathfrak{S})\,k_n(\mathfrak{L})^2}{\left(-1+\cos(\mathfrak{S})\,k_g(\mathfrak{L})+\sin(\mathfrak{S})\,k_n(\mathfrak{L})\right)^2} + \frac{\tau_g'(\mathfrak{L})}{\left(-1+\cos(\mathfrak{S})\,k_g(\mathfrak{L})+\sin(\mathfrak{S})\,k_n(\mathfrak{L})\right)^3}\big((\sin(\mathfrak{S}) + \cos(\mathfrak{S})\sin(\mathfrak{S})\,k_g(\mathfrak{L}) + (-2 + \sin(\mathfrak{S})^2)k_n(\mathfrak{L}))\Bigg)$$

$$\mathcal{K}_{\mathfrak{L}} = \frac{\csc(\mathfrak{S})}{\left(-1+\cos(\mathfrak{S})\,k_g(\mathfrak{L})+\sin(\mathfrak{S})\,k_n(\mathfrak{L})\right)^3} \begin{pmatrix} -2\big(\cos(\mathfrak{S})\,k_g'(\mathfrak{L})+\sin(\mathfrak{S})\,k_n'(\mathfrak{L})\big) \\ \Big(k_n(\mathfrak{L})\begin{pmatrix}-1+\cos(\mathfrak{S})\,k_g(\mathfrak{L})+\\ \sin(\mathfrak{S})\,k_n(\mathfrak{L})\end{pmatrix} - \cos(\mathfrak{S})\,\tau_g'(\mathfrak{L})\Big) + \\ \begin{pmatrix}-1+\cos(\mathfrak{S})\,k_g(\mathfrak{L})\\ +\sin(\mathfrak{S})\,k_n(\mathfrak{L})\end{pmatrix} \\ \begin{pmatrix}\big(-1+\cos(\mathfrak{S})\,k_g(\mathfrak{L})\big)k_n'(\mathfrak{L})+\\ k_n(\mathfrak{L})\begin{pmatrix}\cos(\mathfrak{S})\,k_g'(\mathfrak{L})+\\ 2\sin(\mathfrak{S})\,k_n'(\mathfrak{L})\end{pmatrix} - \cos(\mathfrak{S})\,\tau_g''(\mathfrak{L})\end{pmatrix} \end{pmatrix}$$

$$\mathcal{K}_{\mathfrak{S}} = \frac{\csc(\mathfrak{S})^5}{2\left(\csc(\mathfrak{S}) - \cot(\mathfrak{S})\,k_g(\mathfrak{L}) - k_n(\mathfrak{L})\right)^3}$$

$$\Big(-k_n(\mathfrak{L})\Big(2\cos(\mathfrak{S}) + (\mathrm{Cos}(\mathfrak{S}) + \cos(3\mathfrak{S}))k_g(\mathfrak{L})^2 + \sin(2\mathfrak{S})\,k_n(\mathfrak{L})(-3 + 2\sin(\mathfrak{S})\,k_n(\mathfrak{L}))\Big) + k_g(\mathfrak{L})\big(-1-3\cos(2\mathfrak{S}) + 2\,\sin(3\mathfrak{S})\,k_n(\mathfrak{L})\big) - \tau_g'(\mathfrak{L})(-2 + (\cos(\mathfrak{S}) + \cos(3\mathfrak{S}))k_g(\mathfrak{L}) + (3\sin(\mathfrak{S}) + \sin(3\mathfrak{S}))k_n(\mathfrak{L}))\Big)$$

From the earlier equations we substitute from the equation

$$\mathcal{H}_{\mathfrak{L}}\mathcal{K}_{\mathfrak{S}} - \mathcal{H}_{\mathfrak{S}}\mathcal{K}_{\mathfrak{L}} = 0$$

We get.

$$\tau_g'(\mathfrak{L}) = -\csc(\mathfrak{S})\sec(\mathfrak{S})$$

then we have

$$\tau_g(\mathfrak{L}) = \int -csc(\mathfrak{S})\,sec(\mathfrak{S})\;d\mathfrak{L}$$
$$\tau_g(\mathfrak{L}) = -\mathfrak{L}\,csc(\mathfrak{S})\,sec(\mathfrak{S}) + c$$

This surface $\mathfrak{D}$ is Weingarten.

Theorem 3.5 The sweeping surface $\mathfrak{D}$ according to Darboux frame in isotropic 3-space is a minimal surface if and only if:

$$k_g(\mathfrak{L}) = \frac{1}{2}Tan(\mathfrak{S})^2(2\,cot(\mathfrak{S})\,csc(\mathfrak{S}) - 3\,cot(\mathfrak{S})\,k_n(\mathfrak{L}) \pm cot(\mathfrak{S})\sqrt{k_n(\mathfrak{L})^2 + 4\,cot(\mathfrak{S})\,\tau_g'(\mathfrak{L})}$$

proof: The sweeping surface $\mathfrak{D}$ is minimal surface if and only if $\mathcal{H}(\mathfrak{L},\mathfrak{S}) = 0$ From the Eq. (23)

$$\big(csc(\mathfrak{S})^2 + cot(\mathfrak{S})^2\,k_g(\mathfrak{L})^2 - 3\,csc(\mathfrak{S})\,k_n(\mathfrak{L}) + 2k_n(\mathfrak{L})^2 + cot(\mathfrak{S})\,csc(\mathfrak{S})\,k_g(\mathfrak{L})(-2 + 3\,sin(\mathfrak{S})\,k_n(\mathfrak{L}) - cot(\mathfrak{S})\,\tau_g'(\mathfrak{L})\big) = 0\,,$$

then we get

$$k_g(\mathfrak{L}) = \frac{1}{2}Tan(\mathfrak{S})^2(2\,cot(\mathfrak{S})\,csc(\mathfrak{S}) - 3\,cot(\mathfrak{S})\,k_n(\mathfrak{L}) \pm cot(\mathfrak{S})\sqrt{k_n(\mathfrak{L})^2 + 4\,cot(\mathfrak{S})\,\tau_g'\mathfrak{L})}$$

Then the surface $\mathfrak{D}$ is minimal.

4 Application

An illustrative example is offered as an implementation of our major findings. It's also used to double-check the results of prior calculations.

Application. 1 Let $\mathfrak{D}$ be a surface defined by:

$$\boldsymbol{\chi}(\mathfrak{L},\ \mathfrak{S}) = \{\boldsymbol{Cosh}(\mathfrak{L}), \boldsymbol{Sinh}(\mathfrak{L}) + \boldsymbol{cos}(\mathfrak{S})\,, \boldsymbol{sin}(\mathfrak{S})\} \tag{28}$$

$$\mathfrak{z}_1 = \left(\frac{Sinh(\mathfrak{L})}{\sqrt{Cosh(2\mathfrak{L})}}, \frac{Cosh(\mathfrak{L})}{\sqrt{Cosh(2\mathfrak{L})}}, 0\right)$$

$$\mathfrak{z}_2 = (0,0,1)$$

$$\mathfrak{z}_3 = \begin{pmatrix} \frac{Cosh(\mathfrak{L})Sin(\mathfrak{S})Sinh(\mathfrak{L})}{\sqrt{Cosh(2\mathfrak{L})}\sqrt{cos(\mathfrak{S})^2\,Cosh(\mathfrak{L})^2 + Sinh(\mathfrak{L})^2}}, \\ -\frac{Sin(\mathfrak{S})Sinh(\mathfrak{L})^2}{\sqrt{Cosh(2\mathfrak{L})}\sqrt{cos(\mathfrak{S})^2\,Cosh(\mathfrak{L})^2 + Sinh(\mathfrak{L})^2}}, \\ \frac{cos(\mathfrak{S})\sqrt{Cosh(2\mathfrak{L})}}{\sqrt{cos(\mathfrak{S})^2\,Cosh(\mathfrak{L})^2 + Sinh(\mathfrak{L})^2}} \end{pmatrix}$$

$$k_g(\mathfrak{L}) = \frac{sin(\mathfrak{S})\, Sinh(\mathfrak{L})}{Cosh(2\mathfrak{L})^{3/2}\sqrt{cos(\mathfrak{S})^2\, Cosh(\mathfrak{L})^2 + Sinh(\mathfrak{L})^2}}$$

$$k_n(\mathfrak{L}) = \frac{cos(\mathfrak{S})\, Sech(2\mathfrak{L})}{\sqrt{cos(\mathfrak{S})^2\, Cosh(\mathfrak{L})^2 + Sinh(\mathfrak{L})^2}}$$

$$\tau_g(\mathfrak{L}) = 0$$

The sweeping surface of the parametric function is presented in Figure 1. Moreover, the gradient candy color covers most of the surface is presented in Figure 2 and Figure 3.

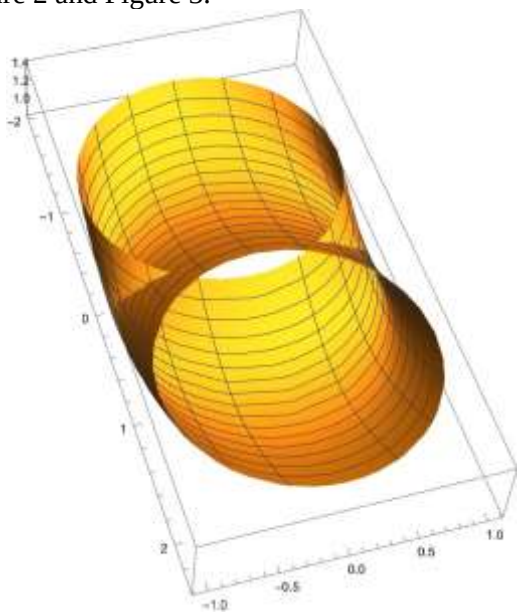

Fig. 1: The sweeping surface of the parametric function (28).

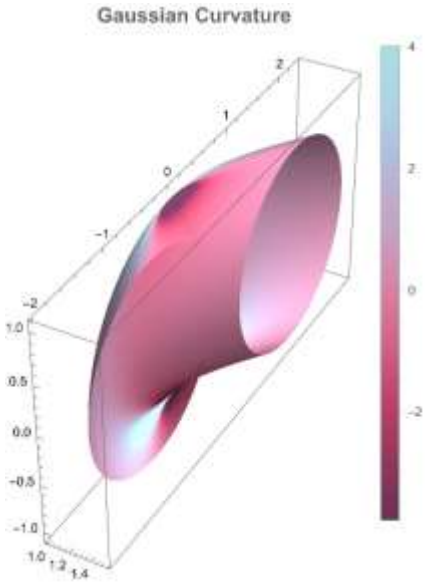

Fig. 2: The gradient candy color covers most of the surface, while the Gaussian curvature increases in the blue color at value 4 and reduces significantly in the purple color at value -2 [see Eq (28)].

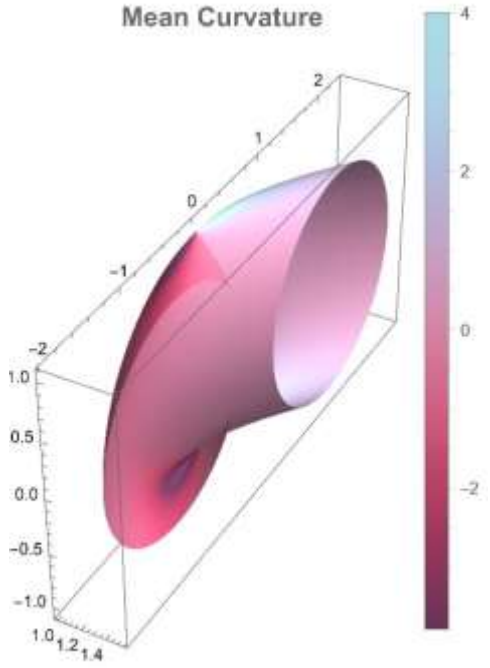

Fig. 3: The gradient candy color covers most of the surface, while the mean curvature increases at value 4 in the light blue color and decreases dramatically at value -2 in the purple color. [see Eq (28)]

Application. 2 Let $\mathfrak{D}$ be a surface defined by:

$$\boldsymbol{\chi}(\mathfrak{L},\, \mathfrak{S}) = (-\mathbf{3}\mathfrak{L} + \mathbf{2}\,, \mathbf{3}\mathfrak{L}^{\mathbf{2}} + \mathfrak{L} + \boldsymbol{cos}(\mathfrak{S})\,, \boldsymbol{sin}(\mathfrak{S})) \tag{29}$$

$$\mathfrak{z}_1 = \left(-\frac{3}{\sqrt{9+(1+6\mathfrak{L})^2}}, \frac{1+6\mathfrak{L}}{\sqrt{9+(1+6\mathfrak{L})^2}}, 0\right)$$

$$\mathfrak{z}_2 = (0,0,1)$$

$$\mathfrak{z}_3 = \left(\frac{-1-6\mathfrak{L}}{\sqrt{2}\sqrt{5+6\mathfrak{L}(1+3\mathfrak{L})}}, -\frac{3}{\sqrt{9+(1+6\mathfrak{L})^2}}, 0\right)$$

$$k_g(\mathfrak{L}) = -\frac{18}{(9+(1+6\mathfrak{L})^2)^{3/2}}$$

$$k_n(\mathfrak{L}) = 0$$

$$\tau_g(\mathfrak{L}) = 0$$

The sweeping surface of the parametric function is presented in Figure 4. Lastly, the curvature is a negative value and our findings are presented in Figure 5 and Figure 6.

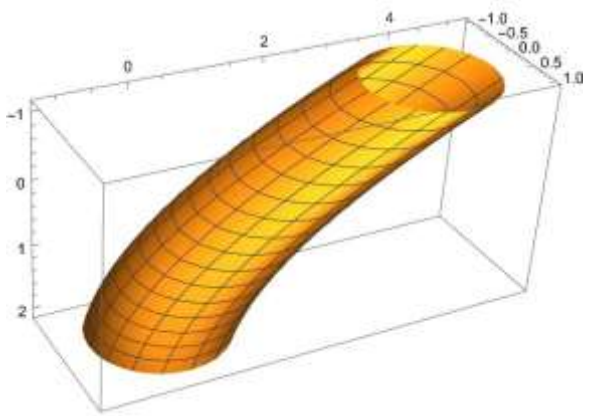

Fig. 4: The sweeping surface of the parametric function (29).

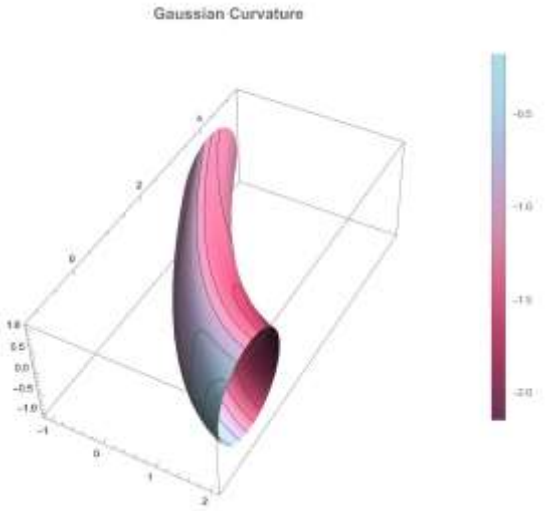

Fig. 5: The curvature is a negative value. Gradation of colors between the most common pink and violet color, the curvature gradually decreases. At the less prevalent light blue hue, the Gaussian curvature increases [see Eq (29)].

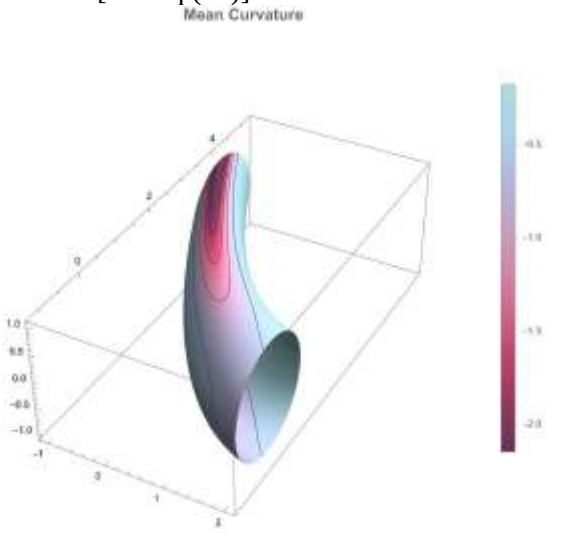

Fig. 6: The curvature is a negative value. It is clear from the drawing that when the light blue color is more widespread, the curvature gradually increases. At the gradient of the less common pink and violet colors, the Gaussian curvature increases [see Eq (29)].

5 Conclusion

In this research, we studied the sweeping surface with an isotropic space using Bishop's framework and knowing the conditions necessary for the sweeping surface to be minimal, developable surface, Weingarten sweeping surface, non-asymptotic curves, non-geodesic curves and we studied the application on the surface and explained the characteristics of the frame in these applications.

Acknowledgments:
The authors would like to convey their heartfelt gratitude to the referee for his/her thorough reading and numerous helpful suggestions for improving the article.

References:

[1] F. Mofarreh, R. A. Abdel-Baky, & N. Alluhaibi, Spacelike sweeping surfaces and singularities in Minkowski 3-space, Mathematical Problems in Engineering, Vol. 2021, January 2021.

[2] Rashad A. Abdel-Baky, Fatemah Mofarreh, "Sweeping Surface of Center Curve on Surface in Euclidean 3-space E^3," WSEAS Transactions on Mathematics, vol. 20, pp. 235-243, 2021.

[3] W. M. Mahmoud, E. M. Soliman, M. A. Solouma, &M. Bary, The new study of some characterization of canal surfaces with weingarten and linear weingarten types according to bishop frame, Journal of the Egyptian Mathematical Society, Vol. 27, No. 1, pp. 1–17, August 2019.

[4] H. Pottmann, & J. Wallner, Computational line geometry, Springer, 2001.

[5] F. Klo , Two moving coordinate frames for sweeping along a 3d trajectory, Computer Aided Geometric Design, Vol. 3 , No.3 , pp. 217–229, November 1986.

[6] R. T. Farouk , C. Giannell , M. L. Sestini , & A. Alessandra , Rotation-minimizing osculating frames, Computer Aided Geometric Design, Vol. 31 ,No. 1, pp. 27–42, January 2014.

[7] Rashad A. Abdel-Bakya, Monia F. Naghi, "Timelike Sweeping Surfaces According to Type-2 Bishop Frame in Minkowski 3–

space," WSEAS Transactions on Mathematics, vol. 19, pp. 555-563, 2020

[8] R. T. Farouki, & T. Sakkalis, Rational rotation-minimizing frames on polynomial space curves of arbitrary degree, Journal of Symbolic computation, Vol. 45, No. 8, pp. 844–856, August 2010.

[9] F. Klok, Two moving coordinate frames for sweeping along a 3d trajectory, Computer Aided Geometric Design, Vol. 3, No.3, pp. 217–229, November 1986.

[10] R. T. Farouki, C. Giannelli , M. L.Sestini , & A. Alessandra , Rotation-minimizing osculating frames, Computer Aided Geometric Design, Vol. 31 ,No. 1, pp. 27–42, January 2014.

[11] N. Gürbüz , & D. W. Yoon, Geometry of curve flows in isotropic spaces, AIMS Mathematics, Vol. 5 No. 4, pp. 3434–3445, April 2020.

[12] M. E. Aydin, & M. Ergüt, Affine translation surfaces in the isotropic 3-space, International Electronic Journal of Geometry, Vol. 10, No.1, pp. 21-30, 2017.

[13] A. O. Ogrenmis, Certain classes of ruled surfaces in 3-dimensional isotropic space, Palestine Journal of Mathematics, Vol. 7, No. 1, PP. 87–91, January 2018.

[14] A. Kelleci, & L. C. da Silva. Invariant surfaces with coordinate finite-type gauss map in simply isotropic space, Journal of Mathematical Analysis and Applications,Vol. 495, No. 1,pp. 124–673, November 2021.

Contribution of Individual Authors to the Creation of a Scientific Article (Ghostwriting Policy)

All the authors contributed significantly to the essay and accept full responsibility for its content. The final manuscript was read and approved by both writers.

Sources of Funding for Research Presented in a Scientific Article or Scientific Article Itself

There is no funding to carry out this research.

Availability of Data and Materials

This paper's data and materials are all freely available.

Conflict of Interest

The authors disclose that no competing interests exist.